frontiers in Materials

ORIGINAL RESEARCH
published: 27 October 2021
doi: 10.3389/fmats.2021.734683

Bioactive 3D Scaffolds for the Delivery of NGF and BDNF to Improve Nerve Regeneration

Ana M. Sandoval-Castellanos, Frederik Claeyssens and John W. Haycock*

Department of Materials Science and Engineering, Biomaterials and Tissue Engineering Group, Kroto Research Institute, The University of Sheffield, Sheffield, United Kingdom

Peripheral nerve injury is an important cause of disability, that can hinder significantly sensory and motor function. The clinical gold standard for peripheral nerve repair is the use of autografts, nevertheless, this method has limitations such as donor site morbidity. An emerging alternative to autografts are nerve guide conduits, which are used to entubulate the severed nerve and provide guidance for the directed regeneration of the nerve tissue. These nerve guide conduits are less effective than autografts, and to enhance their performance the incorporation of neurotrophins can be considered. To enable optimal nerve regeneration, it is important to continuously stimulate neurite outgrowth by designing a delivery system for the sustained delivery of neurotrophins. The aim of this study was to develop a novel bioactive surface on electrospun fibres to supply a sustained release of heparin bound NGF or BDNF electrostatically immobilised onto an amine functionalized surface to encourage neurite outgrowth and Schwann cell migration. The bioactive surface was characterised by XPS analysis and ELISA. To assess the effect of the bioactive surface on electrospun fibres, primary chick embryo dorsal root ganglia were used, and neurite outgrowth and Schwann cell migration were measured. Our results showed a significant improvement regarding nerve regeneration, with the growth of neurites of up to 3 mm in 7 days, accompanied by Schwann cells. We hypothesize that the physical guidance provided by the fibres along the sustained delivery of NGF or BDNF created a stimulatory environment for nerve regeneration. Our results were achieved by immobilising relatively low concentrations of neurotrophins (1 ng/ml), which provides a promising, low-cost, and scalable method to improve current nerve guide conduits.

Keywords: bioactive surface, NGF (nerve growth factor), BDNF (brain derived neurotrophic factor), nerve regeneration, drug delivery, surface coating

OPEN ACCESS

Edited by:
Oliver Goerke,
Technical University of Berlin, Germany

Reviewed by:
Jyothi U. Menon,
University of Rhode Island, United States
Ezgi Antmen,
Massachusetts General Hospital and Harvard Medical School, United States

****Correspondence:***
Frederik Claeyssens
f.claeyssens@sheffield.ac.uk

Specialty section:
This article was submitted to Biomaterials, a section of the journal Frontiers in Materials

Received: *01 July 2021*
Accepted: *12 October 2021*
Published: *27 October 2021*

Citation:
Sandoval-Castellanos AM, Claeyssens F and Haycock JW (2021) Bioactive 3D Scaffolds for the Delivery of NGF and BDNF to Improve Nerve Regeneration. Front. Mater. 8:734683. doi: 10.3389/fmats.2021.734683

1 INTRODUCTION

Peripheral nerve injury affects 2.8% of trauma patients (Manoukian et al., 2019), and the current treatment is the use of autografts (Bozkurt et al., 2007). However, the limitations of using autografts are donor site morbidity, size mismatch, and the need of at least two surgeries (Bozkurt et al., 2007). The use of hollow tubes called nerve guide conduits (NGCs) has been studied as an alternative to aid nerve repair (Pateman et al., 2015; Behbehani et al., 2018; Billet et al., 2019). Nevertheless, NGCs does not support sufficient nerve regeneration in gaps longer than 20 mm (Daly et al., 2012; Pateman et al., 2015; Manoukian et al., 2020). Therefore, the addition of topographical and chemical cues to the NGCs has been studied to improve their performance and, hence, nerve repair.

Research using gradients, aligned multichannels, and aligned/random electrospun scaffolds have demonstrated that an oriented cue can enhance neurite outgrowth as well as Schwann cell migration (Guenard et al., 1992; Daud et al., 2012; Xie et al., 2014; Ren et al., 2015; Bolaina-Lorenzo et al., 2016; Chwalek et al., 2016). For example, Hurtado et al. showed that aligned nanofibers stimulated neurite regrowth in a spinal cord injury model (Hurtado et al., 2011). Furthermore, Kim et al. reported that aligned fibers encouraged neurite growth in a 17 mm sciatic injury (Kim et al., 2008). In addition, studies had stated that the use of aligned electrospun scaffolds would be more beneficial to use as these might resemble the extracellular matrix (ECM) (Hurtado et al., 2011; Xie et al., 2014). Therefore, if Schwann cells are stimulated to migrate (Maniwa et al., 2003; Heermann and Schwab, 2013), these cells and the aligned electrospun scaffold would create a regenerative environment to aid nerve repair (Horne et al., 2010; Daud et al., 2012). Although studies using aligned fibrous scaffold have stimulated neurite outgrowth, the level of nerve regeneration produced is still not sufficient (for example, 2.1 ± 0.33 mm, 1.4 mm), as the critical nerve gap in humans is 4 cm, and in rats is 1.5 cm (Wang et al., 2010; Kaplan et al., 2015; Behbehani et al., 2018). An interesting route to further enable nerve repair is to include chemical cues in the NGCs to provide a long term permissive environment (Chwalek et al., 2016; Liu et al., 2018).

Nerve growth factor (NGF) and brain derived neurotrophic factor (BDNF) are known to encourage neurite outgrowth and Schwann cell migration after nerve injury (Frostick et al., 1998; Fine et al., 2002; Deister and Schmidt, 2006; Matsumoto et al., 2007; Horne et al., 2010; Santos et al., 2016; Yi et al., 2016). Nevertheless, their use in the clinic, and in different approaches, is limited by their half-life, loss of their biological activity and that they might not reach the injury site (DeYoung et al., 2004; Pfister et al., 2008; Liu et al., 2019). Hence, research has been conducted to design and fabricate systems for the delivery of growth factors, which would protect growth factors from degradation and denaturation (Zeng et al., 2014). Growth factors can be incorporated onto electrospun scaffolds by covalent binding, electrostatic interactions, coatings, encapsulation and addition of microspheres, emulsion and coaxial electrospinning (Dinis et al., 2014; Liu et al., 2019). With the exception of surface functionalisation via either covalent binding or electrostatic interactions, all the aforementioned techniques compromise the integrity and functionality of the growth factors due to their use of organic solvents or crosslinking agents (Kuo and Huang, 2012; Whitehead et al., 2018; Ikegami and Ijima, 2020). The effectivity of covalent binding of growth factors has been demonstrated before, for example, Guex et al. covalently immobilised vascular endothelial growth factor (VEGF) onto an oxygen plasma treated scaffold and promoted endothelial cell proliferation (Guex et al., 2014). Nevertheless, covalent binding might result in the loss of bioactivity or denaturation of the growth factor (Willerth and Sakiyama-Elbert, 2007; Robinson et al., 2008; Hajimiri et al., 2015).

A second approach is to use electrostatic interactions to bind growth factors. Indeed, heparin has been used to immobilise growth factors by electrostatic interactions (Robinson et al., 2008; Robinson et al., 2012). For example, Robinson et al. bound osteoprotogerin or tissue inhibitor of metalloproteinases 3 to heparin and studied their release (Robinson et al., 2012). Heparin is highly negatively charged, so to bind heparin to a surface by electrostatic interactions, this surface needs to have a positive charge. Plasma treatment and deposition is commonly used to add charged functional groups to a surface, changing the properties of the surface (Fine et al., 2002; Robinson et al., 2012; Recek et al., 2013). For example, air and oxygen plasma treatment are used to make polymeric surfaces hydrophilic (Recek et al., 2013), and typically renders these surfaces negatively charged (Lehocký, 2003). To produce positively charged surfaces in a polymeric substrate, amine based plasma deposition can be used, for example, by using allylamine to add positively charged amine (NH_2^+) functional groups to a surface (Lee et al., 1994; Fine et al., 2002; Robinson et al., 2012). Hence, the surfaces functionalised by plasma deposited NH_2^+ groups bind heparin, which consequently binds growth factors such as NGF, BDNF or a mixture of NGF and BDNF.

Previously, we showed how a bioactive surface, which was used as a delivery system of growth factors, was fabricated by using electrostatic interactions (Crawford-Corrie et al., 2017; Sandoval-Castellanos et al., 2020). Furthermore, we demonstrated that bioactive surfaces composed of NH_2^+ + Heparin + Immobilised NGF, NH_2^+ + Heparin + Immobilised BDNF, and NH_2^+ + Heparin + Immobilised NGF plus BDNF encouraged neurite outgrowth of chick embryo dorsal root ganglia (DRG) on 2D surfaces (Sandoval-Castellanos et al., 2020).

Therefore, the novelty of this study was to assess the efficiency of this bioactive surface coating onto 3D scaffolds, as the combined action of chemical cues and contact guidance is envisage to further encourage and enhance neurite outgrowth in comparison to 2D surfaces (Roach et al., 2007). Moreover, it is critical to design and scale up this bioactive surface so it can be easily translated into clinical use. Polycaprolactone (PCL) was the chosen material to fabricate these 3D scaffolds due to its bioresorbable properties and for its slow degradation rate, which is up to 4 years (Lam et al., 2008). These properties are advantageous for our bioactive surface, as PCL could sustain the bioactivity of the surface without compromising the structure of the scaffold. Also, PCL is an FDA-approved polyester, which has been used previously for drug delivery and for nerve repair applications (Woodruff and Hutmacher, 2010; Daud et al., 2012; Nectow et al., 2012; Shahriari et al., 2017).

Therefore, electrospinning was used to fabricate a novel 3D bioactive scaffold for nerve regeneration, made from aligned PCL microfibres. Then, NH_2^+ functional groups were added to the scaffold by plasma deposition. Thereafter, heparin was added by passive conjugation and finally, NGF, BDNF or a combination of NGF plus BDNF were immobilised at different concentrations, including 1 pg/ml and 1 ng/ml, which at the best of our knowledge, have not been used before (Li et al., 2017; Ikegami and Ijima, 2020). Hence, PCL + NH_2^+ + Heparin + Immobilised NGF scaffolds, PCL + NH_2^+ + Heparin + Immobilised BDNF scaffolds, and PCL + NH_2^+ + Heparin + Immobilised NGF plus BDNF scaffolds were fabricated. The bioactive surfaces were characterised by XPS and ELISA to confirm the incorporation

of NH_2^+, heparin and NGF or BDNF. Moreover, to study the potential of the bioactive surface on the PCL electrospun scaffolds, DRG were seeded on the scaffolds, and neurite outgrowth and Schwann cell migration were assessed.

2 MATERIALS AND METHODS

2.1 Fabrication of Polycaprolactone Electrospun Scaffolds

A 20% w/v solution of polycaprolactone (PCL, Mn. 80,000 g/mol, Cat. No. 440744, Sigma-Aldrich, United Kingdom) was prepared in a glass container with dichloromethane (DCM, Cat. No. D/1850/17, Fisher Scientific, United Kingdom) as a solvent. The 20% PCL solution was loaded in a 1 ml syringe (Cat. No. 309628 Beckton Dickinson, BD, United Kingdom). A dispensing blunt needle of 20-gauge, (1 inch long, Cat. No. 8001098, Fisnar, United States) was attached to the syringe and then placed in the syringe pump (AL 1000-220, World Precision Instruments, WPI, United Kingdom). A high voltage supply (Genvolt, United Kingdom) was used to set the required voltage. A flow rate of 6 ml/h, voltage of 16–18 kV, distance of 20 cm, and speed of collector of 2,000 rpm were set to obtain an aligned PCL electrospun scaffold.

2.2 Plasma Deposition

2.2.1 Allylamine Plasma Deposition

PCL electrospun scaffolds were placed inside a glass vessel (10.5 cm diameter, 42.0 cm length). Then, the vacuum pump was turned on to evacuate the glass vessel to 8×10^{-3} mBar. Then, the pressure was adjusted to 2.2×10^{-2} mBar by opening the inlet valve, allowing allylamine monomer (Cat. No. 145831, Aldrich, United Kingdom) into the glass vessel. Thereafter, the radio frequency generator (13.56 MHz) was turned on, and the output power adjusted to 10 W. The allylamine plasma deposition process, which creates a blue discharge glow, was left for 10 min. Thereafter, the radiofrequency generator was turned off, the inlet valve was closed, and the scaffolds were left inside the glass vessel for 5 min to allow any remaining NH_2^+ to bind onto the surface. Then, the scaffolds were placed inside a petri dish to avoid any contamination.

2.2.2 Air Plasma Treatment

PCL electrospun scaffolds were modified with air plasma to be used as positive controls. PCL electrospun scaffolds were placed inside the glass vessel and the vacuum pump was turned on to evacuate the glass vessel to 7×10^{-2} mBar. Then, the pressure was adjusted to 1.8×10^{-1} mBar, allowing air into the glass vessel. Thereafter, the radio frequency generator was turned on, and the output power adjusted to 25 W. The air plasma deposition process was left for 2 min.

2.3 Heparin Conjugation to Polycaprolactone + NH_2^+ Scaffolds

A solution of heparin sodium salt (Cat. No. H3393, Sigma, United Kingdom) was prepared at a concentration of 50 µg/ml. This heparin solution was added to the PCL + NH_2^+ scaffolds and incubated overnight at room temperature. After incubation, the heparin solution was discarded. Heparin conjugation was done 24 h after plasma treatment.

2.4 Immobilisation of Nerve Growth Factor, Brain Derived Neurotrophic Factor and Nerve Growth Factor Plus Brain Derived Neurotrophic Factor to Polycaprolactone + NH_2^+ + Heparin Scaffolds

NGF (Cat. No. 556-NG/CF, R&D systems, United States), BDNF (Cat. No. 248-BD/CF, R&D systems, United States) and a combination of both (NGF plus BDNF) were immobilised onto PCL + NH_2^+ + Heparin scaffolds. NGF and BDNF, alone, were prepared at concentrations of 1 pg/ml, 1 ng/ml, 10 ng/ml, 100 ng/ml, and 1 µg/ml. NGF plus BDNF were prepared at concentrations of 1 and 100 ng/ml. Each solution was added onto PCL + NH_2^+ + Heparin scaffolds and incubated for 5 h at room temperature. Then, the solutions were discarded. PCL + NH_2^+ + Heparin + Immobilised NGF scaffolds, PCL + NH_2^+ + Heparin + Immobilised BDNF scaffolds, and PCL + NH_2^+ + Heparin + Immobilised NGF plus BDNF scaffolds were now fabricated.

2.5 Scanning Electron Microscopy Analysis of Polycaprolactone Electrospun Scaffolds

Scanning Electron Microscopy (SEM) was used to obtain images of the PCL electrospun scaffolds to measure the diameter the fibres, before and after plasma deposition. Samples of the PCL electrospun scaffold were cut in 1 cm × 1 cm squares and placed on carbon adhesive tabs (Leit adhesive carbon tabs, Cat. No. AGG3347N, Agar Scientific, United Kingdom). To improve the quality of the image, all samples of PCL electrospun scaffolds were gold-coated (SC 500A, Emscope) before imaging with a field emission SEM (Sorby Centre, FE SEM JSM-6500F, Jeol Ltd., United Kingdom). The voltage used was 10 kV and the spot size was 3.5 nm.

ImageJ 1.52a software (National Institutes of Health, United States) (Schneider et al., 2012) was used to measure the diameter of the fibres in the PCL electrospun scaffold, before and after plasma deposition. Three tests were run independently, and three PCL electrospun scaffolds chosen as samples. Three images were taken, and 10 PCL fibres were measured, per image.

2.6 X-Ray Photoelectron Spectroscopy Analysis of Polycaprolactone + NH_2^+ + Heparin Scaffolds

After 24 h of fabricating the bioactive surface, X-ray Photoelectron Spectroscopy (XPS) analysis was performed at the Sheffield Surface Analysis Centre (The University of Sheffield, United Kingdom). PCL scaffolds were interrogated to determine surface elemental composition (survey scans), nitrogen scans (N 1s), and sulphur scans (S 2p) using a Kratos Ultra instrument with a monochromated aluminium source (1,486.6 eV). Elemental survey scans were collected between 1,200 and 0 eV binding energy, 160 eV pass energy and 1 eV intervals. High resolution

N 1s and S 2p scans were collected at 40 eV pass energy and 0.1 eV intervals. Data was processed and analysed using CasaXPS (version 2.3.19 PR 1.0, Casa Software Ltd).

2.7 Release Profile of Nerve Growth Factor and Brain Derived Neurotrophic Factor for 21 days

The release of NGF and BDNF for 21 days was characterised by ELISA. NGF and BDNF were immobilised at 1 ng/ml following the protocol described in *Immobilisation of Nerve Growth Factor, Brain Derived Neurotrophic Factor and Nerve Growth Factor Plus Brain Derived Neurotrophic Factor to Polycaprolactone + NH_2^+ + Heparin Scaffolds*. Samples were incubated with phosphate buffered saline (PBS; Cat. No. BR0014G, Oxoid, United Kingdom) at 37°C. Samples were taken at 1 h, 24 h, 48 h, 168 h (7 days), 240 h (10 days), 336 h (14 days), 408 h (17 days), and 504 h (21 days) and stored at −20°C for later quantification, following the manufacturer's instructions (NGF and BDNF kit, Cat. No. DY556, DY248, DY008, R&D systems, United States). Four samples were interrogated per test condition. Two independent tests were performed.

2.8 *In vitro* Evaluation Using Chick Embryo Dorsal Root Ganglia

Fertilised brown chicken eggs (Henry Stewart & Co. Ltd., United Kingdom) were incubated at 37.5°C and 50–70% humidity for 12 days (E12). Thereafter, day 12 eggs were opened in a biological safety cabinet to collect the E12 embryo, which was cleaned, and organs were removed [in compliance with UK Home Office Animals (Scientific Procedures) Act 1986 and definition of chicken as a Protected Animal from E14]. DRG were dissected under a dissecting microscope (Wild M3Z, Switzerland) and any remains of the root were cut. DRG were seeded at a density of one per scaffold. DRG were cultured on PCL + NH_2^+ + Heparin + Immobilised NGF scaffolds, PCL + NH_2^+ + Heparin + Immobilised BDNF scaffolds, and PCL + NH_2^+ + Heparin + Immobilised NGF plus BDNF scaffolds with Dulbecco's modified Eagle's medium (DMEM; Cat. No. D6546, Sigma, United Kingdom) plus 10% (v/v) fetal bovine serum (FBS, Cat. No. P30-3,306, PAN Biotech, Germany), 1% (v/v) L-glutamine (Cat. No. G7513, Sigma, United Kingdom), 1% (v/v) penicillin/streptomycin (P/S; Cat. No. P0781, Sigma, United Kingdom), 0.25% (v/v) amphotericin B (Cat. No. A2942, Sigma, United Kingdom). DRG that were seeded on PCL scaffolds, PCL + NH_2^+ scaffolds, and PCL + NH_2^+ + Heparin scaffolds were culture with DMEM supplemented with 10% FBS, 1% P/S, 1% L-glutamine, 0.25% amphotericin B, and 1 μg/ml of NGF or BDNF. Scaffolds with DRG were cultured for 7 days at 37°C and 5% CO_2.

2.9 Immunolabelling of Dorsal Root Ganglia: β-III Tubulin and S100β

Immunolabelling was performed for β-III tubulin protein, to identify neurons and measure neurite outgrowth and S100-β protein to identify Schwann cells. Samples were fixed using 3.7% v/v paraformaldehyde (PFA, Cat. No. 158127, Sigma, United Kingdom). Then, 0.1% v/v Triton X-100 (Cat. No. BP151, Sigma, United Kingdom) with 3% w/v bovine serum albumin solution (BSA, Cat. No. A7030, Sigma, United Kingdom) was added to the samples and incubated for 1 h at room temperature. Primary antibodies, anti-β-III tubulin (1:1,000, Cat. No. ab7751, RRID: AB_306045, Abcam, United Kingdom) and anti-S100β (1:400, Cat. No. Z5116, RRID: AB_2622233, Dako, United States) in 1% w/v BSA solution were added to the samples and incubated overnight at 4°C. Then, the solution was discarded and secondary antibodies, Alexa Fluor 488 goat anti-mouse, and Alexa Fluor 546 goat anti-rabbit (1:400, Cat. No. A-11001 and A-11010, Life technologies, United States) in 1% BSA solution was added and incubated for 3 h at 4°C. The samples were rinsed one time with PBS and then stored at 4°C with PBS. Secondary antibody control groups were imaged to assure that antibodies did not bind nonspecifically (**Supplementary Figure S1**).

2.10 Lightsheet Microscopy

Lightsheet microscopy was used to obtain images of the DRG seeded on bioactive scaffolds. Z.1 lightsheet microscope (Carl Zeiss AG, Germany) and ZEN imaging software (Zen 9.2.8.54, Carl Zeiss, Germany) were used to obtain these images. Samples were cut longitudinally and then mounted in 1% agarose solution (w/v, in dH_2O, Cat. No. A9414, Sigma-Aldrich, United Kingdom) inside glass capillaries (diameter 2.15 mm, Cat. No. 701999, Carl Zeiss AG, Germany). Samples were localised and positioned in front of the objective. The objective used was a Zeiss W Plan-Apochromat 10 × /N.A. 0.5 for detection and two Zeiss LSFM 5 × /N.A. 0.1 for illumination. Alexa Fluor-488 and Alexa Fluor-546 were imaged using excitation and emission wavelengths of λ_{ex} = 488 nm/λ_{em} = 550 nm (short band filter), and λ_{ex} = 561 nm/λ_{em} = 545–590 nm (band pass filter) respectively. For each sample, various fields of view (longitudinally) were taken to capture all neurite outgrowth and Schwann cell migration. Each field of view was imaged in z-stack.

The z-stack was combined to produce a maximum projection intensity image using ZEN lite software (Carl Zeiss, Germany). Then, the maximum projection intensity images were put together using the stitching tool in ImageJ 1.52a software (Preibisch et al., 2009). The straight tool in ImageJ 1.52a software (Schneider et al., 2012) was used to measure neurite outgrowth and Schwann cell migration. Neurites (neurite bundle) were measured from the end of the DRG body to the tip of the neurite. Schwann cells were measured from the end of the DRG body to the last Schwann cell (the one most distal from the DRG). Two images were taken per sample. Three independent tests were performed. Each condition was tested in triplicate.

2.11 Statistical Analysis

Analysis of variance (ANOVA) with Tukey multiple comparison test was performed to analyse statistical difference among the different conditions using GraphPad Prism 8.2.0 software (United States). A p value of <0.05 was used to indicate if differences in data were significant.

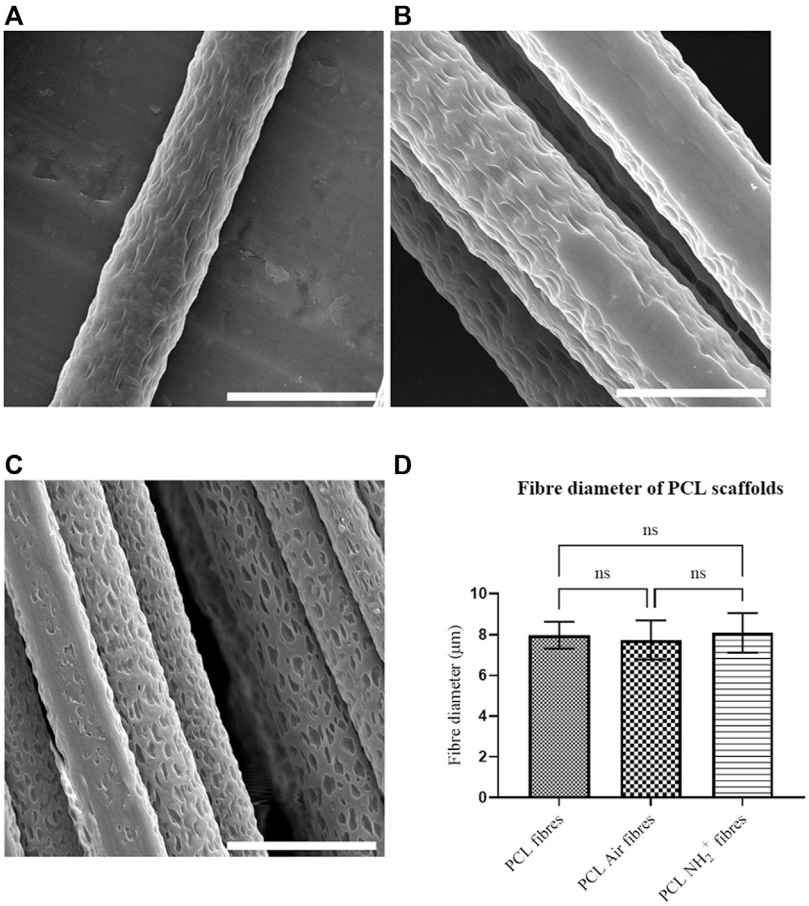

FIGURE 1 | PCL electrospun fibres morphology. **(A)** PCL fibre before plasma deposition; **(B)** PCL fibre after air plasma deposition; **(C)** PCL fibre after allylamine plasma deposition; **(D)** Bar chart showing fibre diameter of PCL fibres before and after plasma deposition, with no significant differences (One-way ANOVA). Scale bar = 10 µm.

3 RESULTS

3.1 Polycaprolactone Fibre Morphology and Diameter Before and After Plasma Deposition Measured via Scanning Electron Microscopy

The fibre diameter of the electrospun scaffold is a critical parameter for *in vitro* neuronal cell migration as highlighted in our previous papers (Daud et al., 2012; Behbehani et al., 2018). The fibre diameter of the non-treated PCL scaffold was measured and compared to the plasma treated scaffolds, either after air plasma treatment or allylamine plasma treatment or deposition. This was mainly to identify if PCL fibres had undergone significant changes after plasma deposition. **Figure 1** presents representative SEM figures of the fibres before and after treatment. The PCL fibres show a wavy surface micro-texture both before and after surface treatment, at a 0.5–1 µm length scale. This texture is likely due to solvent evaporation during the electrospinning process (Yazgan et al., 2017; Xue et al., 2019). Additionally, the diameter of PCL fibres (**Figure 1A**), PCL air plasma treated fibres (**Figure 1B**) and PCL NH_2^+ fibres (**Figure 1C**) was measured to be 8 ± 0.7, 7.7 ± 0.9, and 8.1 ± 0.9 µm, respectively. There was no significant difference between these values, as shown in **Figure 1D**.

3.2 X-Ray Photoelectron Spectroscopy Analysis of Bioactive Polycaprolactone Scaffolds

XPS analysis was performed to confirm the presence of amine NH_2^+ functional groups and heparin (through sulphur detection) in PCL scaffolds. **Table 1** shows the percentage of atomic concentration of PCL scaffolds (**Figure 2A**), PCL Air scaffolds (**Figure 2B**), PCL + NH_2^+ scaffolds (**Figure 2C**), and PCL + NH_2^+ + Heparin scaffolds (**Figure 2D**). Survey scans of the samples showed that nitrogen was introduced after allylamine plasma deposition and that sulphur was detected in PCL + NH_2^+ + Heparin scaffolds, confirming the successful adsorption of heparin on this scaffold. Carbon and oxygen peaks were observed at 285 and 532 eV, respectively. After allylamine plasma deposition, a nitrogen peak at 400 eV was expected to appear on the PCL NH_2^+ scaffolds, which XPS analysis confirmed. In addition, a sulphur peak was detected at 168 eV

TABLE 1 | Percentage of atomic concentration of PCL scaffolds, PCL Air scaffolds, PCL NH_2^+ scaffolds and PCL NH_2^+ + Heparin scaffolds obtained from XPS analysis survey scans. Si content was also detected on the surface.

Sample	Survey scan: percentage atomic concentration %			
	O	N	C	S
PCL scaffolds	23.4 ± 0.7	0 ± 0	70.2 ± 2.4	0 ± 0
PCL air plasma treated scaffolds	26.9 ± 0.4	0 ± 0	72.4 ± 0.4	0 ± 0
PCL + NH_2^+ scaffolds	23.1 ± 2.7	21.2 ± 11.7	54.2 ± 8.3	0 ± 0
PCL + NH_2^+ + Heparin scaffolds	26.0 ± 1.2	7.5 ± 1.1	64.7 ± 2.0	0.2 ± 0

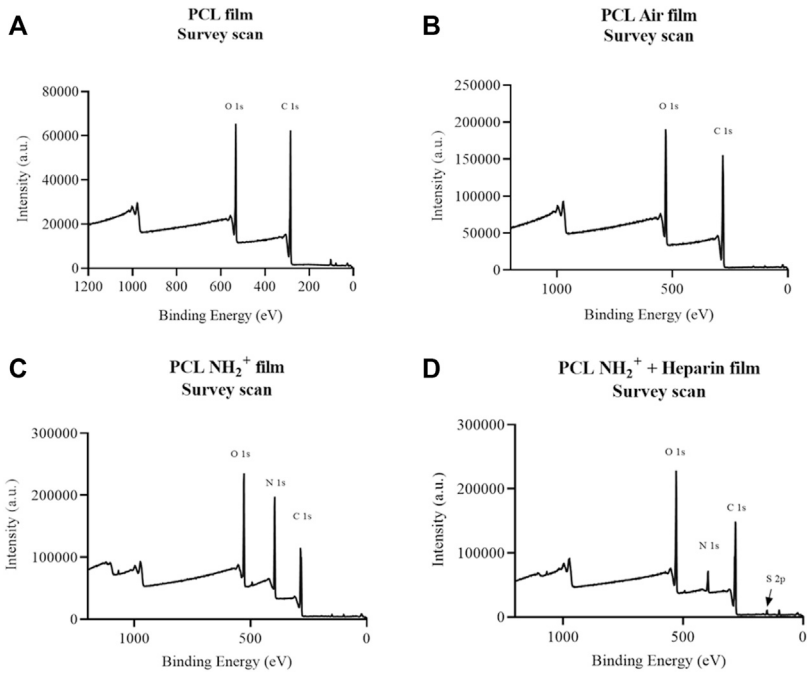

FIGURE 2 | XPS survey scans of **(A)** PCL scaffold; **(B)** PCL air treated scaffold (PCL Air scaffold); **(C)** PCL + NH_2^+ scaffold; **(D)** PCL+ NH_2^+ + Heparin scaffold. Carbon was detected at 285 eV, oxygen at 532 eV, nitrogen at 400 eV, and sulphur at 168 eV.

in the PCL + NH_2^+ + Heparin scaffolds, confirming the presence of heparin on the scaffolds.

N 1s scans of PCL + NH_2^+ scaffolds, and PCL + NH_2^+ + Heparin scaffold, revealed that nitrogen was incorporated to the films. Moreover, two peaks were identified, one at 399 eV, indicating C-N, and a peak at 401 eV, which was attributed to NH_2^+ (Begum et al., 2017). However, overall nitrogen content decreased from 21.2 to 7.5%, after heparin attachment, this could indicate that nitrogen might have been lost after incubation step of heparin or after rinsing step (Dehili et al., 2006). On the other hand, the drop in percentage of nitrogen content can also be attributed to strong binding of heparin to the plasma polymerised allylamine coating. Heparin (with atomic formula $C_{12}H_{19}NO_{20}S_3$) contains only three at %N (excluding H), and a concentration of heparin within the analysis depth of XPS (typically 10 nm) decrease the nitrogen content. Interestingly, the amount of sulphur detected by the survey scan was 0.2 at %, this confirms the electrostatic binding of heparin to the surface. The amount of sulphur on the surface is in line with our previously reported surface concentration of allylamine-heparin coating in tissue culture plastic (Sandoval-Castellanos et al., 2020). Additionally, this is also in line with the figure reported of 0.5 at %S on the surface by layer-by-layer deposition of polyethylene-heparin on a polylactic acid surface (Gigliobianco et al., 2015).

In addition, S 2p scan of PCL + NH_2^+ + Heparin scaffolds revealed two peaks, which were consistent with sulphur present in heparin (OSO_3 and NSO_3) (John et al., 1992; Kristensen et al., 2003; Kristensen et al., 2006). These two peaks correspond to the spin orbit split of S 2p, S $2p^{3/2}$ (168.2 eV) and S $2p^{1/2}$ (169.3 eV). Hence, heparin was adsorbed successfully to the PCL NH_2^+ + Heparin scaffold.

3.3 Nerve Growth Factor and Brain Derived Neurotrophic Factor Release From Bioactive Surfaces

After heparin immobilisation, the surface was treated with NGF or BDNF. ELISA detected the release of NGF and BDNF, for

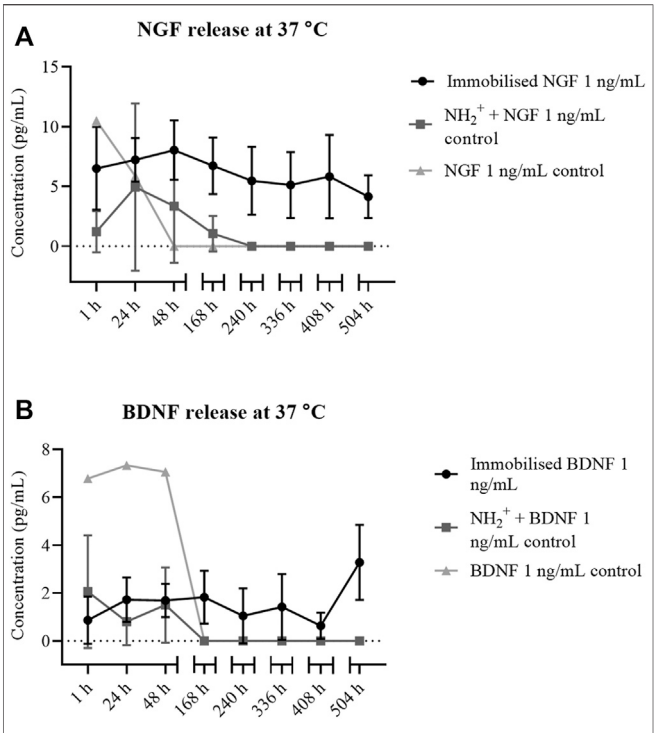

FIGURE 3 | NGF and BDNF release from NH_2^+ + Heparin. **(A)** NH_2^+ + Heparin + Immobilised NGF 1 ng/ml (circles), and NH_2^+ (squares) at different time points, from 1 to 504 h (21 days). NGF at 1 ng/ml in solution in PBS was used as a control (triangles). **(B)** BDNF release from NH_2^+ + Heparin + Immobilised BDNF 1 ng/ml (circles), and NH_2^+ (squares) at different time points, from 1 to 504 h (21 days). BDNF at 1 ng/ml in solution was used as a control (triangles).

21 days, from bioactive surfaces NH_2^+ + Heparin when NGF and BDNF were immobilised, and NH_2^+ scaffolds. **Figure 3** shows the sustained released of NGF and BDNF for 21 days. In contrast, when NGF was added to NH_2^+ surface only, NGF release was observed at 1, 24, 48, and 168 h. After the 168 h time point, no release of NGF was observed. Furthermore, from the control (NGF in PBS), active NGF was not detected after 24 h. Similarly, when BDNF was added to NH_2^+ surface only, BDNF release was observed at 1, 24, and 48 h. After the 48 h time point, no release of BDNF was observed. Furthermore, from the control, active BDNF was not detected after 168 h. This indicates that the immobilisation strategy via binding of the growth factors to heparin allows for a sustained release of active growth factors over an extended time period.

3.4 Dorsal Root Ganglia Neurite Outgrowth and Schwann Cell Migration

Neurite outgrowth of DRG and Schwann cell migration were measured and averaged to obtain average neurite length and average Schwann cell migration of DRG cultured on seven different surface treated scaffolds: 1) PCL scaffolds, 2) PCL air plasma treated scaffolds, 3) PCL + NH_2^+ scaffolds, 4) PCL + NH_2^+ + Heparin scaffolds, 5) PCL + NH_2^+ + Heparin + Immobilised NGF scaffolds, 6) PCL + NH_2^+ + Heparin + Immobilised BDNF scaffolds and 7) PCL + NH_2^+ + Heparin + Immobilised NGF plus BDNF scaffolds.

The longest average neurite length, from the NGF group, was 3,041 ± 843 μm for DRG cultured on PCL + NH_2^+ + Heparin + Immobilised NGF at 1 ng/ml. The shortest average neurite length was 226 ± 177 μm for DRG cultured on PCL scaffolds (**Figure 4A**). The longest Schwann cell migration was 2,718 ± 911 μm when DRG were seeded on immobilised NGF at 1 ng/ml. The shortest migration length of Schwann cells was 270 ± 185 μm when DRG were cultured on PCL scaffolds (**Figure 4B**).

The longest average neurite length from the BDNF group was 1,536 ± 762 μm for when DRG were cultured on PCL + NH_2^+ + Heparin + Immobilised BDNF at 1 ng/ml (**Figure 4C**). The longest Schwann cell migration was 1,614 ± 543 μm when DRG were seeded on PCL + NH_2^+ + Heparin + Immobilised BDNF at 10 ng/ml (**Figure 4D**).

The longest average neurite length and Schwann cell migration from NGF plus BDNF group were 1,816 ± 583, and 1,974 ± 708 μm, respectively, when DRG were cultured on PCL air plasma treated scaffolds with NGF plus BDNF at 1 μg/ml in solution in culture medium (**Figures 4E,F**). Interestingly, these results also showed that the co-immobilisation of NGF and BDNF did not have any accumulative effect and that this combination did not stimulate the growth of longer neurites.

Overall, these results suggested that the delivery of NGF at a relative low concentration of 1 ng/ml as an immobilised neurotrophin from PCL + NH_2^+ + Heparin + Immobilised NGF scaffolds, encouraged the growth of longer neurites, in comparison to the other control and test scaffolds. This delivery system, using NGF at 1 ng/ml would be an appropriate candidate for further studies regarding nerve repair.

These cell culture results were further investigated with an *in vitro* organ culture via placing DRG onto the scaffold. **Figure 5** shows representative lightsheet images of DRG grown on 1) PCL, 2) PCL air plasma treated, 3) PCL + NH_2^+, 4) PCL + NH_2^+ + Heparin, without growth factor, 5) PCL + NH_2^+ + Heparin + Immobilised NGF at 1 ng/ml, 6) PCL + NH_2^+ + Heparin + Immobilised BDNF at 1 ng/ml, and 7) PCL air plasma treated with NGF plus BDNF at 1 μg/ml in culture medium. Neurites were stained for β-III tubulin (green), and Schwann cells were stained for S100β (red). Growing neurites are usually accompanied by migrating Schwann cells, hence, co-localisation of both β-III tubulin and S100β was expected. This co-localisation is observed in yellow.

4 DISCUSSION

We reported on the successful fabrication of bioactive 3D scaffolds for the delivery of NGF, BDNF, or NGF plus BDNF for enhancing nerve repair. PCL fibrous scaffolds were fabricated by electrospinning and fibre diameter was measured using SEM. NH_2^+ functional groups were added by plasma deposition, and heparin was added to fabricate the bioactive surface NH_2^+ + Heparin. Furthermore, NGF and BDNF were successfully immobilised onto the surface via binding to the

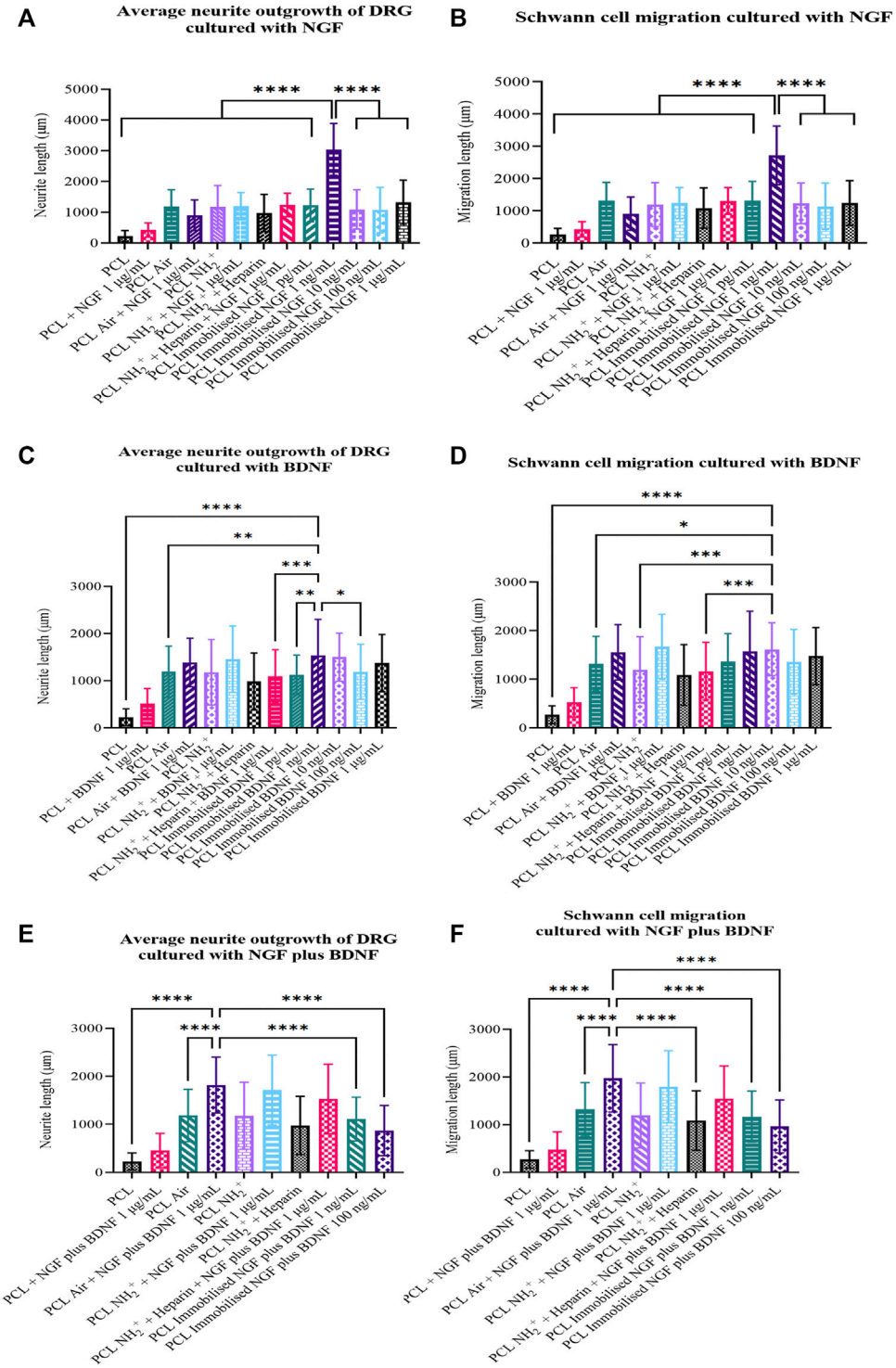

FIGURE 4 | Average neurite length and Schwann cell migration of DRG when cultured on PCL scaffolds, PCL Air scaffolds, PCL + NH_2^+ scaffolds, PCL + NH_2^+ + Heparin scaffolds, and PCL + NH_2^+ + Heparin + Immobilised neurotrophin for 7 days. **(A)** Average neurite length and **(B)** Schwann cell migration for when DRG were cultured with NGF. NGF was immobilised on the bioactive surfaces at 1 pg/ml, 1 ng/ml, 10 ng/ml, 100 ng/ml, and 1 µg/ml. NGF was added in solution at 1 µg/ml with control surfaces. **(C)** Average neurite length and **(D)** Schwann cell migration for when DRG were cultured with BDNF. BDNF was immobilised on the bioactive surfaces at 1 pg/ml, 1 ng/ml, 10 ng/ml, 100 ng/ml, and 1 µg/ml. BDNF was added in solution at 1 µg/ml with control surfaces. **(E)** Average neurite length and **(F)** Schwann cell migration for when DRG were cultured with NGF plus BDNF. NGF plus BDNF were immobilised on the bioactive surfaces at 1 and 100 ng/ml. NGF plus BDNF were added in solution at 1 µg/ml with control surfaces. One-way ANOVA statistical analysis was performed with Tukey procedure of multiple comparisons *p < 0.05, **p < 0.01, ***p < 0.001, ****p < 0.0001.

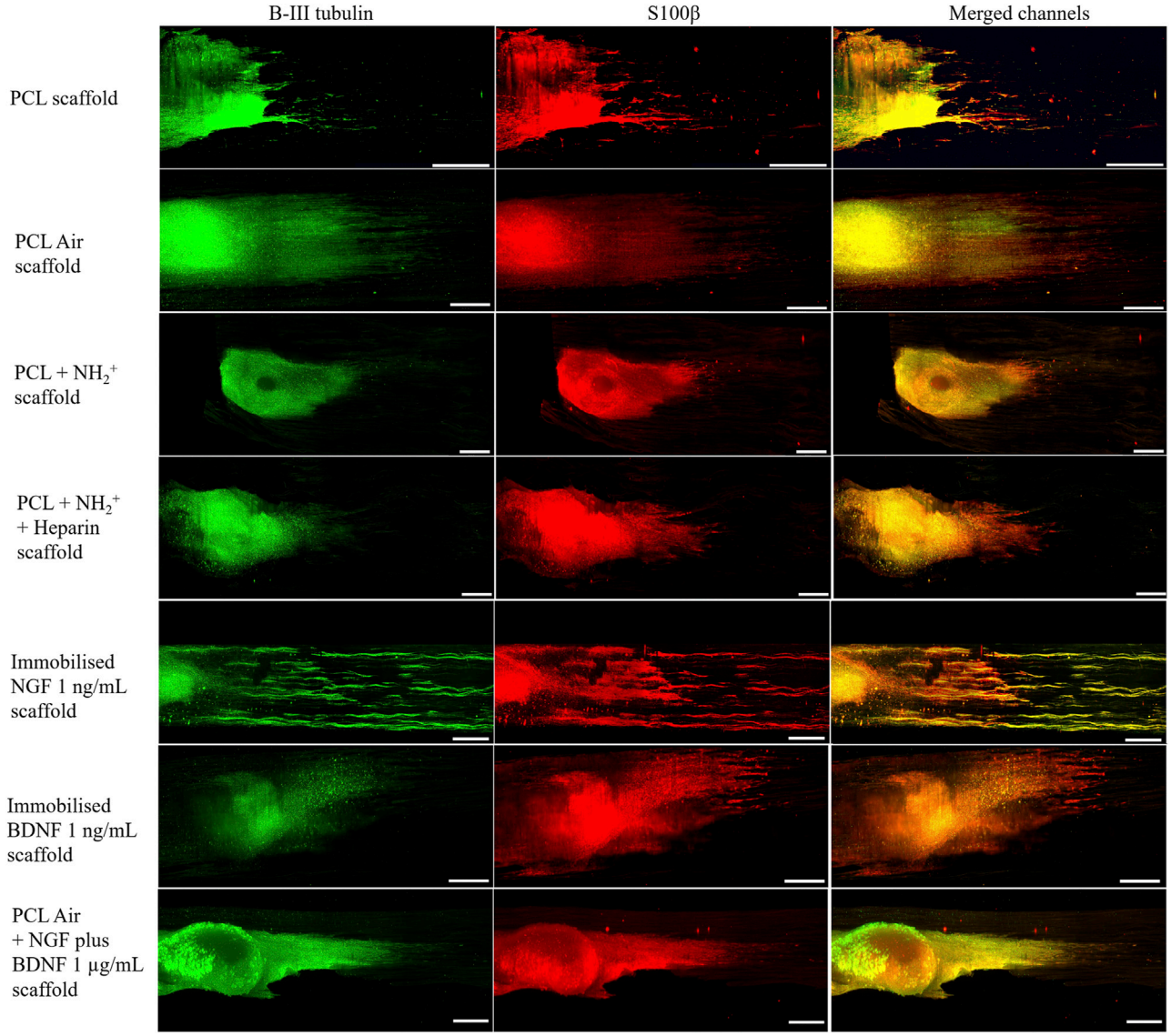

FIGURE 5 | DRG seeded on control PCL bioactive scaffolds: PCL scaffold, PCL air treated scaffold (PCL Air scaffold), PCL + NH_2^+ scaffold, PCL + NH_2^+ + Heparin scaffold, PCL + NH_2^+ + Heparin + Immobilised NGF at 1 ng/ml scaffold, PCL + NH_2^+ + Heparin + Immobilised BDNF at 1 ng/ml scaffold, and PCL air treated scaffold (PCL Air scaffold) with NGF plus BDNF at 1 µg/ml in culture medium. B-III tubulin protein in neurites stained in green. S100β of Schwann cells stained in red. Merged channels are yellow, representing the co-localisation of growing neurites and Schwann cells. Scale bar = 500 µm.

electrostatically immobilised heparin. The addition of NH_2^+ and heparin was confirmed by XPS. Moreover, the addition of NGF or BDNF and its release were confirmed by ELISA. Culture of primary chick embryo DRG was used to assess the effects of the bioactive scaffolds. Furthermore, cell viability was assessed on the bioactive surface by MTS assay (**Supplementary Figure S2**), where no decrease in metabolic activity was observed.

Research has been conducted to study how scaffolds with aligned structures can improve neurite outgrowth to aid nerve repair. Daud et al. fabricated PCL electrospun scaffold (8 µm fibre diameter) and seeded DRG on them to evaluate neurite outgrowth and Schwann cell migration. This study showed that, after 10 days in culture, Schwann cells migrated 1.9 mm and that neurite outgrowth was 1.6 mm (Daud et al., 2012). Additionally, Bozkurt et al. fabricated a parallel-oriented pores scaffold using collagen and evaluated neurite outgrowth from DRG. This study revealed that maximum and average neurite outgrowth, after 21 days in culture, was 1,496, and 756 µm respectively (Bozkurt et al., 2007). Moreover, Behbehani et al. fabricated PCL fibres and introduced them inside a polyethylene glycol conduit. Neurite outgrowth and Schwann cell migration from DRG seeded on this construct were 2.1 and 2.2 mm respectively, after 21 days in culture (Behbehani et al., 2018). Furthermore, Hurtado et al. fabricated random and aligned poly-L-lactic acid (PLLA) fibres and measured neurite length developed by DRG after 5 days in culture. This study showed

that random PLLA fibres encouraged neurite growth of ca. 900 and 800 μm (maximum and average neurite length respectively), whereas aligned PLLA fibres promoted neurite growth of ca. 1,700 and 1,500 μm (maximum and average neurite length respectively) (Hurtado et al., 2011).

These studies showed that even if different materials can be used as guidance, and the alignment and fibre diameter and density can be controlled, these features alone are not sufficient to induce rapid cell attachment and neurite outgrowth, which is needed for nerve repair (Ramsey et al., 1984; Meek and Coert, 2008; Kehoe et al., 2012). Therefore, it is important to improve these strategies to encourage the growth of longer neurites.

Plasma deposition technique is usually used to add functional groups onto surfaces of materials to modify surface properties, such as surface energy and wettability (Chan et al., 1996; Recek et al., 2013). Indeed, hydrophobic surfaces can be produced via using fluorine containing compounds for plasma treatment, while hydrophilic surfaces can be obtained via using oxygen or nitrogen containing plasmas (Chan et al., 1996; Recek et al., 2013). Plasma treatment and polymerisation has been used to improve cell adhesion, proliferation, and to add functional groups to further modify the surface of a material. Furthermore, functional groups have been introduced by plasma polymerisation onto the surface of a material to bind growth factors, thus allowing the delivery of the growth factor in a sustained manner to encourage a specific cell response. For example, Guex et al. functionalised PCL fibrous scaffolds via plasma treatment with carbon dioxide, ethene, and argon. Then, VEGF was covalently immobilised onto the activated PCL scaffold (Guex et al., 2014). This study showed that proliferation of endothelial cells was improved when VEGF was immobilised on the surface (Guex et al., 2014). Furthermore, Shen et al. evaluated that adhesion and proliferation of fibroblast was improved by the immobilisation of basic fibroblast growth factor (bFGF) on carbon dioxide plasma treated poly(lactide-co-glycolyde) (PLGA) films (Shen et al., 2008).

Therefore, allylamine plasma deposition was performed to fabricate bioactive surfaces of NH_2^+ + Heparin + Immobilised NGF/BDNF/NGF plus BDNF on PCL electrospun scaffolds, to translate this technology for future applications into medical devices to aid nerve repair. Allylamine monomer was used during plasma deposition to add amine functional groups onto PCL fibres. As amine functional groups, NH_2^+, have a positive charge (Robinson et al., 2012), heparin, a negatively charged molecule, will be bound to amine by electrostatic interactions (Robinson et al., 2012). Although the presence of NH_2^+ was detected on the bioactive surface by XPS analysis, how to control the deposition of NH_2^+ bound to the surface, and how different plasma deposition parameters might change the amount of NH_2^+, is yet to be studied in future work.

Crystal violet adhesion assay was performed to evaluate any changes in cell adhesion. The results showed that PCL + NH_2^+ and PCL + NH_2^+ + Heparin scaffolds increased attachment by 76 and 121% in comparison to positive control tissue culture plastic (TCP). In contrast, PCL scaffolds decreased cell attachment by 18% in comparison to TCP (**Supplementary Figure S3**).

NGF and BDNF were immobilised on this bioactive scaffold PCL + NH_2^+ + Heparin. ELISA was performed to confirm the presence of NGF and BDNF on the fabricated NH_2^+ + Heparin scaffold. Moreover, ELISA was also performed to assess the delivery of NGF and BDNF from the bioactive surface within 21 days.

The results from ELISA revealed the controlled release of NGF and BDNF from the surface for up to 21 days. Moreover, it showed that a sustained delivery of both growth factors, with no burst released, was achieved. When NGF and BDNF were bound to NH_2^+ scaffold, NGF and BDNF release was seen within 7 days and 48 h respectively. After that, no growth factor release was observed. This could be due to a very low quantity of growth factors bound to the surface by weak interactions, the degradation of NGF and BDNF because they were not established (Lam et al., 2001). These findings are supported by Kim et al. who found that microspheres loaded with heparin bound significantly more bFGF and NGF than microspheres without heparin (Kim et al., 2015). Moreover, Johnson et al. also incorporated heparin into hydrogels to stabilise both NGF and BDNF (Johnson et al., 2015). This suggests that NH_2^+ + Heparin bioactive scaffold is an appropriate delivery system for the release of NGF and BDNF for 21 days, as it can bind higher quantities of growth factors and stabilise them.

Currently, there is not a defined standard release profile of growth factors to obtain a desired cellular response. This cellular response should be evaluated for each delivery system. For nerve repair, there are two desirable outcomes: encouragement neurite growth and Schwann cell migration. Schwann cells create an environment to stimulate neurite growth and formation. Moreover, neurotrophic factors are produced, by neurite outgrowth and Schwann cell stimulation, to aid both neurite outgrowth and Schwann cell migration (Frostick et al., 1998; Cheng and Zochodne, 2002; Daud et al., 2012; Shakhbazau et al., 2012; Ren et al., 2015; Santos et al., 2016; Yi et al., 2016). Hence, both neurite outgrowth and Schwann cell migration were assessed in this study.

As NGF and BDNF are known to encourage neurite outgrowth in DRG (Matsumoto et al., 2007), both growth factors were immobilised, alone and in combination, on the bioactive surface NH_2^+ + Heparin described herein. This bioactive surface was added to PCL electrospun scaffolds, as the fibres would direct neurite growth and Schwann cell migration. The results showed that PCL + NH_2^+ + Heparin + Immobilised NGF 1 ng/ml encouraged the longest average neurite length and furthest Schwan cell migration (3,041 ± 843 and 2,718 ± 911 μm respectively, for 7 days in culture). PCL + NH_2^+ + Heparin + Immobilised BDNF 1 ng/ml also stimulated neurite outgrowth and Schwann cell migration (1,536 ± 762 μm, 1,571 ± 828 μm respectively), but not as high as the ones encouraged by immobilised NGF. Interestingly, PCL + NH_2^+ + Heparin + Immobilised NGF plus BDNF did not promote comparable neurite outgrowth (1,107 ± 456 μm) and Schwann cell migration (1,169 ± 538 μm) when compared to immobilised NGF 1 ng/ml and immobilised BDNF 1 ng/ml.

Growth factors, specifically neurotrophins, are crucial to enhance neurite outgrowth and Schwann cell migration.

However, due to the half-life of the growth factors, it is essential to design a system which stabilises and delivers growth factors with the purpose of extending the half-life of growth factors, and hence reducing the amount required, and to maintain a sustained delivery of these during the healing process. Liu et al. fabricated micropatterned channels scaffold with polydimethyl-siloxane (PDMS) (Liu et al., 2018). Then, DRG were co-cultured with Schwann cells for 21 days to study neurite outgrowth. Moreover, Liu et al. encapsulated NGF (50 μg/ml) in a collagen gel, which then was incorporated into one of the sides of the PDMS channels. Neurite outgrowth was ca. 2,000 and ca. 2,500 μm respectively for both DRG seeded with Schwann cells and collagen-loaded NGF (Liu et al., 2018).

Additionally, Dinis et al. added NGF and CNTF (1 μg/ml and 100 ng/ml respectively) into a 9% silk fibroin in polyethylene oxide to produce electrospun aligned fibres. When DRG were cultured for 5 days on NGF and CNTF silk fibres, neurite outgrowth was of ca. 1,000–1,500 μm (Dinis et al., 2014). This study partially supported the findings herein, where the use of two growth factors did not have an accumulative effect on neurite outgrowth. Nevertheless, its effect was better than when one of the growth factors was used individually, in this case, CNTF. Furthermore, Whitehead et al. electrospun aligned methacrylated hyaluronic acid with PLGA microspheres, which contained NGF at 100 μg/ml (Whitehead et al., 2018). This study revealed that, after culturing DRG for 5 days, 40–80% of NGF was released from the microspheres, encouraging neurite outgrowth of ca. 1,500–2000 μm (Whitehead et al., 2018).

In contrast, the bioactive scaffold reported herein, PCL + NH_2^+ + Heparin + Immobilised NGF 1 ng/ml encouraged 3,041 ± 843 μm neurite growth and 2,718 ± 911 μm Schwann cell migration from DRG cultured for 7 days. This outcome showed that our bioactive scaffold used as a delivery system optimised the use of NGF and achieved a greater outcome than the ones reported in current literature. PCL + NH_2^+ + Heparin + Immobilised BDNF also stimulated neurite outgrowth, but its growth was not as long as the neurite outgrowth reached when immobilising NGF. Moreover, our results showed that PCL + NH_2^+ + Heparin + Immobilised NGF plus BDNF, although it also promoted neurite outgrowth, it might not be the best combination of growth factors to co-immobilise to obtain a significant neurite outgrowth and Schwann cell migration.

In comparison to our previous work (Sandoval-Castellanos et al., 2020), adding the bioactive surface NH_2^+ + Heparin + Immobilised NGF/BDNF onto PCL electrospun scaffolds significantly stimulated neurite outgrowth and Schwann cell migration. This might be due to the combination of two elements: 1) topographical cues (PCL electrospun scaffold) as these encourage enhanced neurite outgrowth (Kim et al., 2008); and 2) chemical cues (bioactive surface) as it is known that by adjusting the surface properties, cell behaviour, such as adhesion, proliferation, and migration, is enhanced (Ren et al., 2015; Min et al., 2021). Therefore, combining PCL electrospun scaffold with the bioactive surface NH_2^+ + Heparin + Immobilised NGF/BDNF could create a permissive environment, which would mimic up to a certain extent the ECM, to further improve neurite growth and guidance, as well as Schwann cell migration to aid nerve repair.

NGF and BDNF immobilised alone are promising approaches to encourage neurite growth and Schwann cell migration after injury. The reason why DRG were stimulated significantly by immobilised NGF more than BDNF might be related to the number of high affinity receptors present in the DRG (Kimpinski et al., 1997; Maniwa et al., 2003). It is known that in an adult DRG, 40–50% of the receptors are tyrosine kinase receptor (Trk) A, 5–30% are TrkB, and 10–20% are TrkC (Kimpinski et al., 1997). As NGF binds to TrkA and BDNF binds to TrkB, the possibility to stimulate a response with NGF was higher. Moreover, NGF and BDNF also bind to the low affinity receptor $p75^{NTR}$, therefore, NGF and BDNF would be also competing for this receptor, suggesting that an equilibrium of interactions between TrkA and $p75^{NTR}$ or TrkB and $p75^{NTR}$ (Kimpinski et al., 1997) should be achieved to maximise neurite length and Schwann cell migration. In addition, immobilisation of NGF plus BDNF did not show any accumulative effect. In fact, when DRG were seeded on PCL + NH_2^+ + Heparin + Immobilised NGF plus BDNF 1 ng/ml and PCL + NH_2^+ + Heparin + Immobilised NGF plus BDNF 100 ng/ml, average neurite length was 1,107 ± 456 and 867 ± 524 μm respectively. Interestingly, both values are lower than when DRG were seeded with either NGF or BDNF alone at 1 and 100 ng/ml. A possible explanation for this outcome is related to the receptors TrkA, TrkB and $p75^{NTR}$. As mentioned before, an equilibrium of interactions between TrkA/B and $p75^{NTR}$ is required to maximise neurite length. However, as both NGF and BDNF are present, an equilibrium between TrkA, TrkB and $p75^{NTR}$ was expected. Nevertheless, from our results we hypothesised that the receptors were saturated, and the pathway that enables neurite outgrowth was hindered. This needs to be tested further, to clarify why the cumulative effect was not observed.

As mentioned before, sensory neurons (DRG) express more TrkA receptors, whereas motor neurons express more TrkB receptors (Frostick et al., 1998; Min et al., 2021). The advantage of this application is that PCL + NH_2^+ + Heparin + Immobilised NGF uses a relatively low concentration of NGF (1 ng/ml) to encourage longer neurite length. Additionally, it could potentially stimulate the growth of longer neurites in a sensory nerve, encouraging nerve repair. However, a limitation of this application is that PCL + NH_2^+ + Heparin + Immobilised BDNF and PCL + NH_2^+ + Heparin + Immobilised NGF plus BDNF did not stimulate longer neurite outgrowth in sensory neurons. Nevertheless, these scaffolds should be tested further with a motor neuron model and with sensory neurons in combination with motor neurons to fully evaluate the potential of the bioactive surface when both motor and sensory neurons are used.

5 CONCLUSION

The bioactive surfaces NH_2^+ + Heparin + Immobilised NGF, NH_2^+ + Heparin + Immobilised BDNF, and NH_2^+ + Heparin + Immobilised NGF plus BDNF were successfully added onto PCL

electrospun scaffolds. XPS analysis confirmed the presence of NH_2^+ and heparin on the scaffolds. Moreover, ELISA revealed that NGF and BDNF were immobilised on the surface and that a sustained release of both NGF and BDNF was maintained for 21 days. This was a major step, as the bioactive surfaces were successfully added onto PCL electrospun scaffold, representing a step closer to translating this technology into an NGC for future clinical use.

Most importantly, PCL + NH_2^+ + Heparin + Immobilised NGF at 1 ng/ml encouraged the average neurite outgrowth 3,041 ± 843 μm, average maximum neurite length 3,869 ± 1,092 μm, and Schwann cell migration length 2,718 ± 911 μm. To the best of our knowledge, these outcomes have the highest neurite length to NGF ratio found in the literature. This suggests that by immobilising a relatively low concentration of NGF, 1 ng/ml, onto the bioactive surface NH_2^+ + Heparin on PCL electrospun scaffolds, the growth of longer neurites and the further migration of Schwann cells can be achieved. Therefore, these scaffolds PCL + NH_2^+ + Heparin + Immobilised NGF at 1 ng/ml are a promising approach to improve current NGCs to aid nerve repair.

DATA AVAILABILITY STATEMENT

The raw data supporting the conclusion of this article will be made available by the authors, without undue reservation.

AUTHOR CONTRIBUTIONS

Conceptualization, AS-C, FC, JH; Formal analysis, AS-C; Methodology and Investigation, AS-C; Supervision, FC, JH; Writing—original draft, AS-C; Writing—review and editing, FC.

FUNDING

The authors thank CONACyT for financially supporting AS-C. We wish to acknowledge the Henry Royce Institute for Advanced Materials, funded through EPSRC grants EP/R00661X/1, EP/S019367/1, EP/P02470X/1, and EP/P025285/1, for the financial support and Lightsheet access at The University of Sheffield.

ACKNOWLEDGMENTS

The authors thank Deborah Hammond for contribution on the XPS study.

SUPPLEMENTARY MATERIAL

The Supplementary Material for this article can be found online at: https://www.frontiersin.org/articles/10.3389/fmats.2021.734683/full#supplementary-material

REFERENCES

Begum, H., Ahmed, M. S., and Jeon, S. (2017). New Approach for Porous Chitosan-Graphene Matrix Preparation through Enhanced Amidation for Synergic Detection of Dopamine and Uric Acid. *ACS Omega* 2 (6), 3043–3054. doi:10.1021/acsomega.7b00331

Behbehani, M., Glen, A., Taylor, C. S., Schuhmacher, A., Claeyssens, F., and Haycock, J. W. (2018). Pre-Clinical Evaluation of Advanced Nerve Guide Conduits Using a Novel 3D *In Vitro* Testing Model. *Int. J. Bioprint* 4 (1). doi:10.18063/IJB.v4i1.123

Billet, F., Caillaud, M., Richard, L., Vallat, J.-M., and Desmoulière, A. (2019). Peripheral Nerve Regeneration and Intraneural Revascularization. *Neural Regen. Res.* 14 (1), 24–33. doi:10.4103/1673-5374.243699

Bolaina-Lorenzo, E., Martínez-Ramos, C., Monleón-Pradas, M., Herrera-Kao, W., Cauich-Rodríguez, J. V., and Cervantes-Uc, J. M. (2016). Electrospun Polycaprolactone/Chitosan Scaffolds for Nerve Tissue Engineering: Physicochemical Characterization and Schwann Cell Biocompatibility. *Biomed. Mater.* 12 (1), 015008. doi:10.1088/1748-605X/12/1/015008

Bozkurt, A., Brook, G. A., Moellers, S., Lassner, F., Sellhaus, B., Weis, J., et al. (2007). *In Vitro* Assessment of Axonal Growth Using Dorsal Root Ganglia Explants in a Novel Three-Dimensional Collagen Matrix. *Tissue Eng.* 13 (12), 2971–2979. doi:10.1089/ten.2007.0116

Chan, C. M., Ko, T. M., and Hiraoka, H. (1996). Polymer Surface Modification by Plasmas and Photons. *Surf. Sci. Rep.* 24 (1–2), 1–54. doi:10.1016/0167-5729(96)80003-3

Cheng, C., and Zochodne, D. W. (2002). *In Vivo* proliferation, Migration and Phenotypic Changes of Schwann Cells in the Presence of Myelinated Fibers. *Neuroscience* 115, 321–329. doi:10.1016/S0306-4522(02)00291-9

Chwalek, K., Dening, Y., Hinüber, C., Brünig, H., Nitschke, M., and Werner, C. (2016). Providing the Right Cues in Nerve Guidance Conduits: Biofunctionalization versus Fiber Profile to Facilitate Oriented Neuronal Outgrowth. *Mater. Sci. Eng. C* 61, 466–472. doi:10.1016/j.msec.2015.12.059

Crawford-Corrie, J. W., Buttle, D. J., and Haycock, J. (2017). *Haycock, "Medical Implant*. WO 2017/017425 A1.

Daly, W., Yao, L., Zeugolis, D., Windebank, A., and Pandit, A. (2012). A Biomaterials Approach to Peripheral Nerve Regeneration: Bridging the Peripheral Nerve gap and Enhancing Functional Recovery. *J. R. Soc. Interf.* 9 (67), 202–221. doi:10.1098/rsif.2011.0438

Daud, M. F. B., Pawar, K. C., Claeyssens, F., Ryan, A. J., and Haycock, J. W. (2012). An Aligned 3D Neuronal-Glial Co-Culture Model for Peripheral Nerve Studies. *Biomaterials* 33, 5901–5913. doi:10.1016/j.biomaterials.2012.05.008

Dehili, C., Lee, P., Shakesheff, K. M., and Alexander, M. R. (2006). Comparison of Primary Rat Hepatocyte Attachment to Collagen and Plasma-Polymerised Allylamine on Glass. *Plasma Process. Polym.* 3 (6–7), 474–484. doi:10.1002/ppap.200500169

Deister, C., and Schmidt, C. E. (2006). Optimizing Neurotrophic Factor Combinations for Neurite Outgrowth. *J. Neural Eng.* 3 (2), 172–179. doi:10.1088/1741-2560/3/2/011

DeYoung, L. R., Xanthe, M. F., Nguyen, T., and Powell, M. F. (1997). *Stabilizing Formulation for NGF, CA2234231 A1*.

Dinis, T. M., Vidal, G., Jose, R. R., Vigneron, P., Bresson, D., Fitzpatrick, V., et al. (2014). Complementary Effects of Two Growth Factors in Multifunctionalized Silk Nanofibers for Nerve Reconstruction. *PLoS One* 9 (10), e109770. doi:10.1371/journal.pone.0109770

Fine, E. G., Decosterd, I., Papaloïzos, M., Zurn, A. D., and Aebischer, P. (2002). GDNF and NGF Released by Synthetic Guidance Channels Support Sciatic Nerve Regeneration across a Long gap. *Eur. J. Neurosci.* 15, 589–601. doi:10.1046/j.1460-9568.2002.01892.x

Frostick, S. P., Yin, Q., and Kemp, G. J. (1998). Schwann Cells, Neurotrophic Factors, and Peripheral Nerve Regeneration. *Microsurgery* 18 (7), 397–405. doi:10.1002/(SICI)1098-2752

Gigliobianco, G., Chong, C. K., and Macneil, S. (2015). Simple Surface Coating of Electrospun Poly-L-Lactic Acid Scaffolds to Induce Angiogenesis. *J. Biomater. Appl.* 30 (1), 50–60. doi:10.1177/0885328215569891

Guenard, V., Kleitman, N., Morrissey, T., Bunge, R., and Aebischer, P. (1992). Syngeneic Schwann Cells Derived from Adult Nerves Seeded in Semipermeable

Guidance Channels Enhance Peripheral Nerve Regeneration. *J. Neurosci.* 12 (9), 3310–3320. doi:10.1523/jneurosci.12-09-03310.1992

Guex, A. G., Hegemann, D., Giraud, M. N., Tevaearai, H. T., Popa, A. M., Rossi, R. M., et al. (2014). Covalent Immobilisation of VEGF on Plasma-Coated Electrospun Scaffolds for Tissue Engineering Applications. *Colloids Surf. B: Biointerfaces* 123, 724–733. doi:10.1016/j.colsurfb.2014.10.016

Hajimiri, M., Shahverdi, S., Kamalinia, G., and Dinarvand, R. (2015). Growth Factor Conjugation: Strategies and Applications. *J. Biomed. Mater. Res.* 103, 819–838. doi:10.1002/jbm.a.35193

Heermann, S., and Schwab, M. H. (2013). Molecular Control of Schwann Cell Migration Along Peripheral Axons. *Cell Adhes. Migration* 7 (1), 18–22. doi:10.4161/cam.22123

Horne, M. K., Nisbet, D. R., Forsythe, J. S., and Parish, C. L. (2010). Three-Dimensional Nanofibrous Scaffolds Incorporating Immobilized BDNF Promote Proliferation and Differentiation of Cortical Neural Stem Cells. *Stem Cell Dev.* 19 (6), 843–852. doi:10.1089/scd.2009.0158

Hurtado, A., Cregg, J. M., Wang, H. B., Wendell, D. F., Oudega, M., Gilbert, R. J., et al. (2011). Robust CNS Regeneration After Complete Spinal Cord Transection Using Aligned Poly-L-Lactic Acid Microfibers. *Biomaterials* 32 (26), 6068–6079. doi:10.1016/j.biomaterials.2011.05.006

Ikegami, Y., and Ijima, H. (2020). Development of Heparin-Conjugated Nanofibers and a Novel Biological Signal by Immobilized Growth Factors for Peripheral Nerve Regeneration. *J. Biosci. Bioeng.* 129 (3), 354–362. doi:10.1016/j.jbiosc.2019.09.004

John, K. D. B., Moulder, F., Stickle, W. F., and Sobol, P. E. (1992). *Handbook of X-ray Photoelectron Spectroscopy*. Eden Prairie, MN: Perkin-Elmer Corporation.

Johnson, B. N., Lancaster, K. Z., Zhen, G., He, J., Gupta, M. K., Kong, Y. L., et al. (2015). 3D Printed Anatomical Nerve Regeneration Pathways. *Adv. Funct. Mater.* 25, 6205–6217. doi:10.1002/adfm.201501760

Kaplan, H. M., Mishra, P., and Kohn, J. (2015). The Overwhelming Use of Rat Models in Nerve Regeneration Research May Compromise Designs of Nerve Guidance Conduits for Humans. *J. Mater. Sci. Mater. Med.* 26 (8), 226. doi:10.1007/s10856-015-5558-4

Kehoe, S., Zhang, X. F., and Boyd, D. (2012). FDA Approved Guidance Conduits and Wraps for Peripheral Nerve Injury: A Review of Materials and Efficacy. *Injury* 43 (5), 553–572. doi:10.1016/j.injury.2010.12.030

Kim, T. H., Oh, S. H., An, D. B., Lee, J. Y., and Lee, J. H. (2015). Dual Growth Factor-Immobilized Microspheres for Tissue Reinnervation: *In Vitro* and Preliminaryin Vivostudies. *J. Biomater. Sci. Polym. Edition* 26, 322–337. doi:10.1080/09205063.2015.1008882

Kim, Y.-t., Haftel, V. K., Kumar, S., and Bellamkonda, R. V. (2008). The Role of Aligned Polymer Fiber-Based Constructs in the Bridging of Long Peripheral Nerve Gaps. *Biomaterials* 29 (21), 3117–3127. doi:10.1016/j.biomaterials.2008.03.042

Kimpinski, K., Campenot, R. B., and Mearow, K. (1997). Effects of the Neurotrophins Nerve Growth Factor, Neurotrophin-3, and Brain-Derived Neurotrophic Factor (BDNF) on Neurite Growth from Adult Sensory Neurons in Compartmented Cultures. *J. Neurobiol.* 33 (4), 395–410. doi:10.1002/(SICI)1097-4695

Kristensen, E. M. E., Larsson, R., Sánchez, J., Rensmo, H., Gelius, U., and Siegbahn, H. (2006). Heparin Coating Durability on Artificial Heart Valves Studied by XPS and Antithrombin Binding Capacity. *Colloids Surf. B: Biointerf.* 49 (1), 1–7. doi:10.1016/j.colsurfb.2006.02.007

Kristensen, E., Rensmo, H., Larsson, R., and Siegbahn, H. (2003). Characterization of Heparin Surfaces Using Photoelectron Spectroscopy and Quartz Crystal Microbalance. *Biomaterials* 24 (23), 4153–4159. doi:10.1016/S0142-9612(03)00297-7

Kuo, Y.-C., and Huang, M.-J. (2012). Material-driven Differentiation of Induced Pluripotent Stem Cells in Neuron Growth Factor-Grafted Poly(ε-Caprolactone)-Poly(β-Hydroxybutyrate) Scaffolds. *Biomaterials* 33 (23), 5672–5682. doi:10.1016/j.biomaterials.2012.04.046

Lam, C. X. F., Savalani, M. M., Teoh, S.-H., and Hutmacher, D. W. (2008). Dynamics of *In Vitro* Polymer Degradation of Polycaprolactone-Based Scaffolds: Accelerated versus Simulated Physiological Conditions. *Biomed. Mater.* 3 (3), 034108. doi:10.1088/1748-6041/3/3/034108

Lam, X. M., Duenas, E. T., and Cleland, J. L. (2001). Encapsulation and Stabilization of Nerve Growth Factor into Poly(lactic-co-glycolic) Acid Microspheres. *J. Pharm. Sci.* 90 (9), 1356–1365. doi:10.1002/jps.1088

Lee, J. H., Jung, H. W., Kang, I.-K., and Lee, H. B. (1994). Cell Behaviour on Polymer Surfaces with Different Functional Groups. *Biomaterials* 15 (9), 705–711. doi:10.1016/0142-9612(94)90169-4

Lehocký, M. (2003). Plasma Surface Modification of Polyethylene. *Colloids Surf. A Physicochem. Eng. Asp.* 222 (1–3), 125–131. doi:10.1016/S0927-7757(03)00242-5

Li, G., Xiao, Q., Zhang, L., Zhao, Y., and Yang, Y. (2017). Nerve Growth Factor Loaded Heparin/chitosan Scaffolds for Accelerating Peripheral Nerve Regeneration. *Carbohydr. Polym.* 171, 39–49. doi:10.1016/j.carbpol.2017.05.006

Liu, C., Kray, J., and Chan, C. (2018). Schwann Cells Enhance Penetration of Regenerated Axons into Three-Dimensional Microchannels. *Tissue Eng. Regen. Med.* 15 (3), 351–361. doi:10.1007/s13770-018-0115-0

Liu, Y., Yu, S., Gu, X., Cao, R., and Cui, S. (2019). Tissue-engineered Nerve Grafts Using a Scaffold-independent and Injectable Drug Delivery System: A Novel Design with Translational Advantages. *J. Neural Eng.* 16 (3), 036030. doi:10.1088/1741-2552/ab17a0

Maniwa, S., Iwata, A., Hirata, H., and Ochi, M. (2003). Effects of Neurotrophic Factors on Chemokinesis of Schwann Cells in Culture. *Scand. J. Plast. Reconstr. Surg. Hand Surg.* 37 (1), 14–17. doi:10.1080/alp.37.1.14.17

Manoukian, O. S., Arul, M. R., Rudraiah, S., Kalajzic, I., and Kumbar, S. G. (2019). Aligned Microchannel Polymer-Nanotube Composites for Peripheral Nerve Regeneration: Small Molecule Drug Delivery. *J. Controlled Release* 296, 54–67. doi:10.1016/j.jconrel.2019.01.013

Manoukian, O. S., Baker, J. T., Rudraiah, S., Arul, M. R., Vella, A. T., Domb, A. J., et al. (2020). Functional Polymeric Nerve Guidance Conduits and Drug Delivery Strategies for Peripheral Nerve Repair and Regeneration. *J. Controlled Release* 317, 78–95. doi:10.1016/j.jconrel.2019.11.021

Matsumoto, K., Sato, C., Naka, Y., Kitazawa, A., Whitby, R. L. D., and Shimizu, N. (2007). Neurite Outgrowths of Neurons with Neurotrophin-Coated Carbon Nanotubes. *J. Biosci. Bioeng.* 103 (3), 216–220. doi:10.1263/jbb.103.216

Meek, M. F., and Coert, J. H. (2008). US Food and Drug Administration/Conformit Europe-Approved Absorbable Nerve Conduits for Clinical Repair of Peripheral and Cranial Nerves. *Ann. Plast. Surg.* 60 (1), 110–116. doi:10.1097/SAP.0b013e31804d441c

Min, Q., Parkinson, D. B., and Dun, X. P. (2021). Migrating Schwann Cells Direct Axon Regeneration Within the Peripheral Nerve Bridge. *Glia* 69 (2), 235–254. doi:10.1002/glia.23892

Nectow, A. R., Marra, K. G., and Kaplan, D. L. (2012). Biomaterials for the Development of Peripheral Nerve Guidance Conduits. *Tissue Eng. B: Rev.* 18 (1), 40–50. doi:10.1089/ten.teb.2011.0240

Pateman, C. J., Harding, A. J., Glen, A., Taylor, C. S., Christmas, C. R., Robinson, P. P., et al. (2015). Nerve Guides Manufactured from Photocurable Polymers to Aid Peripheral Nerve Repair. *Biomaterials* 49, 77–89. doi:10.1016/j.biomaterials.2015.01.055

Pfister, L. A., Alther, E., Papaloïzos, M., Merkle, H. P., and Gander, B. (2008). Controlled Nerve Growth Factor Release from Multi-Ply Alginate/chitosan-Based Nerve Conduits. *Eur. J. Pharmaceutics Biopharmaceutics* 69 (2), 563–572. doi:10.1016/j.ejpb.2008.01.014

Preibisch, S., Saalfeld, S., and Tomancak, P. (2009). Globally Optimal Stitching of Tiled 3D Microscopic Image Acquisitions. *Bioinformatics* 25 (11), 1463–1465. doi:10.1093/bioinformatics/btp184

Ramsey, W. S., Hertl, W., Nowlan, E. D., and Binkowski, N. J. (1984). Surface Treatments and Cell Attachment. *In Vitro* 20 (10), 802–808. doi:10.1007/BF02618296

Recek, N., Jaganjac, M., Kolar, M., Milkovic, L., Mozetič, M., Stana-Kleinschek, K., et al. (2013). Protein Adsorption on Various Plasma-Treated Polyethylene Terephthalate Substrates. *Molecules* 18 (10), 12441–12463. doi:10.3390/molecules181012441

Ren, T., Yu, S., Mao, Z., and Gao, C. (2015). A Complementary Density Gradient of Zwitterionic Polymer Brushes and NCAM Peptides for Selectively Controlling Directional Migration of Schwann Cells. *Biomaterials* 56, 58–67. doi:10.1016/j.biomaterials.2015.03.052

Roach, P., Eglin, D., Rohde, K., and Perry, C. C. (2007). Modern Biomaterials: a Review-Bulk Properties and Implications of Surface Modifications. *J. Mater. Sci. Mater. Med.* 18 (7), 1263–1277. doi:10.1007/s10856-006-0064-3

Robinson, D. E., Buttle, D. J., Short, R. D., McArthur, S. L., Steele, D. A., and Whittle, J. D. (2012). Glycosaminoglycan (GAG) Binding Surfaces for Characterizing GAG-Protein Interactions. *Biomaterials* 33 (4), 1007–1016. doi:10.1016/j.biomaterials.2011.10.042

Robinson, D. E., Marson, A., Short, R. D., Buttle, D. J., Day, A. J., Parry, K. L., et al. (2008). Surface Gradient of Functional Heparin. *Adv. Mater.* 20 (6), 1166–1169. doi:10.1002/adma.200702586

Sandoval-Castellanos, A. M., Claeyssens, F., and Haycock, J. W. (2020). Biomimetic Surface Delivery of NGF and BDNF to Enhance Neurite Outgrowth. *Biotechnol. Bioeng.* 117 (10), 3124–3135. doi:10.1002/bit.27466

Santos, D., Gonzalez-Perez, F., Navarro, X., and Del Valle, J. (2016). Dose-Dependent Differential Effect of Neurotrophic Factors on *In Vitro* and *In Vivo* Regeneration of Motor and Sensory Neurons. *Neural Plasticity* 2016, 1–13. doi:10.1155/2016/4969523

Schneider, C. A., Rasband, W. S., and Eliceiri, K. W. (2012). NIH Image to ImageJ: 25 Years of Image Analysis. *Nat. Methods* 9 (7), 671–675. doi:10.1038/nmeth.2089

Shahriari, D., Shibayama, M., Lynam, D. A., Wolf, K. J., Kubota, G., Koffler, J. Y., et al. (2017). Peripheral Nerve Growth Within a Hydrogel Microchannel Scaffold Supported by a Kink-Resistant Conduit. *J. Biomed. Mater. Res.* 105 (12), 3392–3399. doi:10.1002/jbm.a.36186

Shakhbazau, A., Kawasoe, J., Hoyng, S. A., Kumar, R., van Minnen, J., Verhaagen, J., et al. (2012). Early Regenerative Effects of NGF-Transduced Schwann Cells in Peripheral Nerve Repair. *Mol. Cell Neurosci.* 50, 103–112. doi:10.1016/j.mcn.2012.04.004

Shen, H., Hu, X., Bei, J., and Wang, S. (2008). The Immobilization of Basic Fibroblast Growth Factor on Plasma-Treated Poly(lactide-Co-Glycolide). *Biomaterials* 29 (15), 2388–2399. doi:10.1016/j.biomaterials.2008.02.008

Wang, H. B., Mullins, M. E., Cregg, J. M., McCarthy, C. W., and Gilbert, R. J. (2010). Varying the Diameter of Aligned Electrospun Fibers Alters Neurite Outgrowth and Schwann Cell Migration. *Acta Biomater.* 6 (8), 2970–2978. doi:10.1016/j.actbio.2010.02.020

Whitehead, T. J., Avila, C. O. C., and Sundararaghavan, H. G. (2018). Combining Growth Factor Releasing Microspheres Within Aligned Nanofibers Enhances Neurite Outgrowth. *J. Biomed. Mater. Res.* 106 (1), 17–25. doi:10.1002/jbm.a.36204

Willerth, S. M., and Sakiyama-Elbert, S. E. (2007). Approaches to Neural Tissue Engineering Using Scaffolds for Drug Delivery. *Adv. Drug Deliv. Rev.* 59 (4–5), 325–338. doi:10.1016/j.addr.2007.03.014

Woodruff, M. A., and Hutmacher, D. W. (2010). The Return of a Forgotten Polymer-Polycaprolactone in the 21st century. *Prog. Polym. Sci.* 35 (10), 1217–1256. doi:10.1016/j.progpolymsci.2010.04.002

Xie, J., Liu, W., Macewan, M. R., Bridgman, P. C., and Xia, Y. (2014). Neurite Outgrowth on Electrospun Nanofibers with Uniaxial Alignment: The Effects of Fiber Density, Surface Coating, and Supporting Substrate. *ACS Nano* 8 (2), 1878–1885. doi:10.1021/nn406363j

Xue, J., Wu, T., Dai, Y., and Xia, Y. (2019). Electrospinning and Electrospun Nanofibers: Methods, Materials, and Applications. *Chem. Rev.* 119 (8), 5298–5415. doi:10.1021/acs.chemrev.8b00593

Yazgan, G., Dmitriev, R. I., Tyagi, V., Jenkins, J., Rotaru, G.-M., Rottmar, M., et al. (2017). Steering Surface Topographies of Electrospun Fibers: Understanding the Mechanisms. *Sci. Rep.* 7 (1), 1–13. doi:10.1038/s41598-017-00181-0

Yi, S., Yuan, Y., Chen, Q., Wang, X., Gong, L., Liu, J., et al. (2016). Regulation of Schwann Cell Proliferation and Migration by MIR-1 Targeting Brain-Derived Neurotrophic Factor after Peripheral Nerve Injury. *Sci. Rep.* 6 (1), 1–10. doi:10.1038/srep29121

Zeng, W., Rong, M., Hu, X., Xiao, W., Qi, F., Huang, J., et al. (2014). Incorporation of Chitosan Microspheres into Collagen-Chitosan Scaffolds for the Controlled Release of Nerve Growth Factor. *PLoS One* 9 (7), e101300. doi:10.1371/journal.pone.0101300

Conflict of Interest: The authors declare that the research was conducted in the absence of any commercial or financial relationships that could be construed as a potential conflict of interest.

Publisher's Note: All claims expressed in this article are solely those of the authors and do not necessarily represent those of their affiliated organizations, or those of the publisher, the editors and the reviewers. Any product that may be evaluated in this article, or claim that may be made by its manufacturer, is not guaranteed or endorsed by the publisher.